

# Fabrication of Poly (Diallyldimethylammonium Chloride) (PDDA) Functionalized Multi-Walled Carbon Nanotubes Paper Electrode for Simultaneous Detection of Dopamine and Ascorbic Acid

Tze-Sian Pui<sup>1\*</sup>, Than Aung<sup>1</sup>, Song Wei Loo<sup>1</sup> and Yuan-Li Hoe<sup>1</sup>

Nanyang Technological University, Singapore

\*Corresponding author: Pui Tze Sian, Nanyang Technological University, Singapore, Email: tspui@ntu.edu.sg

## Research Article

Volume 4 Issue 3

Received Date: December 01, 2019

Published Date: December 10, 2019

DOI: 10.23880/nnoa-16000169

## Abstract

A paper-based electrode based on nanocomposite, comprising of carboxylated multi-walled carbon nanotubes (MWNTs) and poly (diallyldimethylammonium chloride) (PDDA), has been successfully developed for simultaneous detection of dopamine (DA) and ascorbic acid (AA) in 0.1 M phosphate buffer solution (PBS). The fabrication of PDDA/MWNTs electrodes involves two steps: PDDA absorbed onto the surface of carboxylated MWNTs and drop-casting the aqueous mixture of PDDA/MWNTs onto the paper. The electrode size was defined by a window cut into a laminating film. Differential pulse voltammetry was performed with DA concentration ranging from 2  $\mu\text{M}$  to 500  $\mu\text{M}$  in the presence of 1 mM AA. On the surface of PDDA/MWNTs electrode, DA and AA were oxidized respectively at distinguishable potential of 0.156 and -0.068 V (vs. Ag/AgCl). The detection limit of DA was estimated to be 0.8  $\mu\text{M}$ . This nanocomposite electrode has potential application in bioanalysis and biomedicine.

**Keywords:** Dopamine; Differential Pulse Voltammetry; Paper Sensor; Carbon Nanotube

## Introduction

Dopamine (DA) is one of the most important neurotransmitters and plays a vital role in the mammalian central nervous, cardiovascular, renal and hormonal systems [1-3]. Parkinson's disease, schizophrenia and depression occur at very low level of DA concentration [4-6]. Therefore, the development of a sensitive and selective method for determination of DA

molecules is highly desirable for diagnostic research. It is well known that DA possess high electrochemical activity [7,8]. The detection of DA using differential pulse voltammetry (DPV) methods has been widely reported due to their low cost [9], rapid analysis and high sensitivity. However, the co-existence of ascorbic acid (AA) in blood samples with a concentration of 100 – 1000 times higher than that of DA as well as similar oxidation potentials make their simultaneous detection with high

selectivity and sensitivity very challenging [10]. Many studies reported that detection of DA directly with plain electrodes, such as carbon and metallic electrodes is not robust enough to clearly separate the signals of DA and AA [11,12].

Recently, carbon nanomaterials have attracted considerable attention for their potential usage in a wide range of applications because of their unique chemical, electrical, optical and mechanical properties [13-17]. Among the carbon nanomaterials, carbon nanotube (CNT) has been particularly attractive as a novel platform for DA sensing. Viry, et al. demonstrated that carbon nanotube (CNT) fiber microelectrode (CNTFM) could detect DA in the excess of AA [18]. This is because the surface of CNT provides an electrostatic barrier towards AA while enhances attraction of DA via  $\pi$ - $\pi$  interaction. Oxygen-plasma treated CNT electrode has also been reported to be useful in the selective detection of DA [9]. Many studies have been conducted for simultaneous detection of DA and AA, using chemically modified electrodes [19-21]. Do, et al. demonstrated the detection of DA concentration range from 5  $\mu$ M to 177  $\mu$ M at Nafion/single wall carbon nanotube (poly(3-methylthiophene) modified glass carbon electrodes [10]. Such electrode exhibited good electron mediating behavior with well separated oxidation peaks ( $\sim$ 200) for AA and DA. Zhang, et al. [21] reported on the use of multilayer films of shortened multi-walled CNT (MWNTs) assembling on glass carbon electrode with poly(diallyldimethylammonium chloride) (PDDA) for detecting low DA concentration in the presence of higher AA concentration. It showed that PDDA could adsorb onto negatively charge (acid oxidized) CNTs via electrostatic interaction. Such (PDDA/MWNT)<sub>5</sub>/GC electrode had good electrocatalytic activity for both DA and AA.

The nanocomposites-based electrodes have shown improved sensitivity and selectively towards detection of DA. However, fabricating these electrodes involve multiple complicated processing steps and the assay requires large volumes of samples. Investigation for finding a simple, mass-scalable devices at an affordable cost that can discriminate the oxidation of DA from the coexisting molecules is continuing. Paper-based sensors are a new alternative technology for fabricating simple, low-cost and disposable analytical devices [22-24].

In this study, a paper-based electrode was developed using a new nanocomposite material comprised of carboxylated MWNTs and PDDA drop-casting onto a filter paper for simultaneous electrochemical detection of DA

and AA. The preparation involves two simple steps; carboxylated MWNTs was first dispersed with PDDA in deionized (DI) water. Subsequently, the aqueous mixture of PDDA/MWNTs was drop-casted onto a filter paper. The electrode size was defined by a small opening window cut into a laminating film. This paper based PDDA/MWNTs electrode offers simultaneous detection of DA and AA with high sensitivity and selectivity, and thus good potential for practical applications.

## Materials and Methods

### Chemicals

Dopamine, ascorbic acid, potassium ferricyanide ( $K_3[Fe(CN_6)]$ ) and potassium ferrocyanide ( $K_4[Fe(CN_6)]$ ) were purchased from Sigma-Aldrich and were used as received. Aqueous solutions of DA, AA and potassium ferricyanide/ferrocyanide were prepared afresh at the time of experiments in phosphate buffer (PBS, pH 7.4). Carboxylated MWNTs (MWNT-COOH) with an average diameter of 9.5 nm, length 1.5  $\mu$ m and >8% carboxylic acid functionalized, and PDDA were purchased from Sigma-Aldrich. Filter paper grade No.1 was purchased from Whatman (Carolina Biological, NC, USA). Fabric crayons (Crayola, USA) were obtained from local book shop and used for drawing wax patterns on paper. Electric paint was obtained from Bare Conductive (London, United Kingdom).

### Preparation of Carboxylated Mwnts Conductive Ink

The carboxylated MWNT conductive ink was prepared by dispersing 35 mg of carboxylic acid functionalized MWNTs in 35 ml of deionized (DI) water and sonicated for 45 mins. The final concentration of the prepared carboxylated MWNTs was about 1 mg/ml.

### Preparation Of PDDA/Mwnts Nanocomposite

An 35 mg of carboxylated MWNTs was taken in a conical flask, and 32.5 ml of deionized (DI) water was added to it. To this solution, 14.3 wt% (2.5 ml) of PDDA was added. This mixture was then sonicated for 45 mins. Upon sonication, a homogeneous black solution was obtained which indicates the complete dispersion of sample.

### Sensor Fabrication

Working electrodes on the paper were fabricated using simple custom stencil masks (Figure 1). First, both

sides of the filter paper were covered by wax using a fabric crayon. The fabric crayon is a stick of colored wax and nontoxic. It is used to hydrophobize paper. The paper was then baked on a hot plate at 130°C for 3 mins, allowing the wax to diffuse through the porous paper and creating hydrophobicity throughout the thickness of the paper. For the fabrication, a 100 µm thick of clear vinyl application transfer tape, which was previously patterned using a knife-plotter (Silhouette Cameo 3, USA), was fixed on one side of the paper. Afterwards, the electric paint was spread uniformly. Next, the stencil mask was peeled

off. This process creates stencil patterned electric paint lines on the paper.

Subsequently, the patterned paper was laid in the laminating film and heat-sealed by the laminator (Leitz ILAM Home office A4, Finland). Windows were cut into the laminating film by a knife-plotter to define the diameter of the working electrodes (4 mm in diameter). Afterwards, 4 µl of 1 mg/ml of carboxylated MWNTs or PDDA/MWNTs solution was deposited on the opening window of working electrode and then dried at 130°C for 60 seconds.

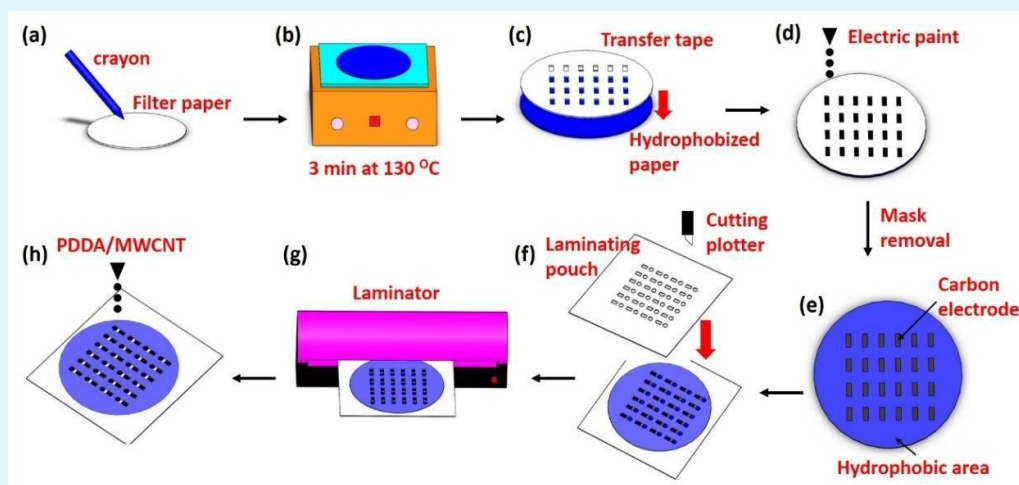


**Figure 1:** Development of PDDA/MWNTs paper electrodes. (a) Both sides of the filter paper are covered with wax using a fabric crayon; (b) The wax on the front side and back side of the paper is melted by placing the paper for 1.5 min on a hot plate at 130°C, respectively; (c) A clear vinyl application transfer tape was cut based on a designed CAD file and then transferred onto hydrophobized paper; (d) Electric paint is spread uniformly onto the hydrophobized paper; (e) The transfer tape is peeled off from the paper and carbon electrodes are well defined on it; (f) The patterned paper is assembled in the laminating film which windows are cut to define the diameter of the working electrodes (4 mm); (g) Sealing the patterned paper using heat-seal laminator; (h) A drop of PDDA/MWNTs solution is deposited onto the opening windows of working electrodes. Subsequently, post-processing of the deposited mixture is done in a hot plate for 60 seconds at 130°C.

## Electrochemical Methods

Differential pulse voltammetry (DPV) and cyclic voltammetry (CV) were performed using the CHI 660 D electrochemical workstation (CH Instrument Company) in a custom-built test cell (Figure 2a). All the electrochemical measurements were performed in a standard three-electrode format at room temperature. The carboxylated MWNTs or PDDA/MWNT paper electrodes were acting as working electrodes (4 mm in diameter). A platinum rod was acting as counter electrode. A sintered Ag/AgCl (A-M, system #550008) wire that was immersed in the

measurement buffer solution acted as a reference electrode. 10 mM PBS (1x, pH 7.4) containing 5 mM  $[(CN)_6]^{-3/-4}$  were used for electrochemical characterization via cyclic voltammetry at a scan rate of 50 mV s<sup>-1</sup>. DPV were recorded by applying potential over the range from -0.2 to 0.4 V, pulse amplitude 50 mV, pulse width 0.05 s and pulse period 0.5 s. To calibrate the PDDA/MWNTs paper electrode response towards DA, 10 µl of the buffer solution (1x PBS, in the presence of 1 mM AA) added with an increase of DA concentration was put into the chamber and incubated for 1 min. Peaks height

for the DA oxidation was then recorded. The concentration of DA was quantified by calculating the change of oxidation peak currents  $\Delta I$  ( $\Delta I = I_o - I$ ), where  $I_o$  was the oxidation peak current without and with DA, respectively. Similar procedures were also carried out to

calibrate the PDDA/MWNTs paper electrode towards AA. The buffer solution (1x PBS, in the presence of 20  $\mu\text{l}$  DA) added with an increase of AA was put into the chamber and incubated for 1 min.

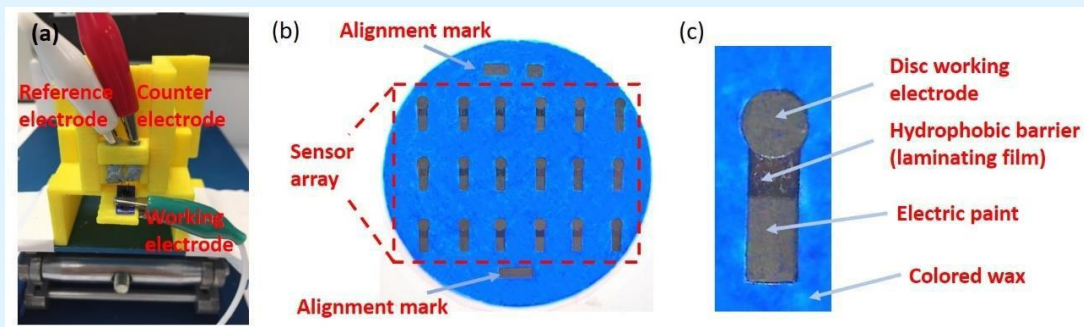


**Figure 2:** Pictures of the electrochemical sensor: (a) sensor mounted on the testing jig; (b) Optical image of working electrode array on a 90 mm diameter filter paper; (c) PDDA/MWNTs disc working electrode (4 mm diameter) which is surrounded by colored wax and a hydrophobic barrier on top.

## Results and Discussion

### Morphology

Figure 2b depicts the optical image of an array of paper electrodes (6 x 3 array) containing 18 small PDDA/MWNT working electrodes, and each electrode is 4 mm in diameter. The electrodes are surrounded by colored wax. Post-treatment of the wax at 130°C makes the paper hydrophobic, as the wax melted into the paper drastically reduces its absorbance properties. Figure 2c depicts a typical zoom-in optical image of the PDDA/MWNTs working electrode that is electrically addressable by electric paint line. A laminating film with a

small opening window is bonded to the paper, and thus delineating the active area of working electrodes.

The morphology and structure of carboxylated MWNTs and PDDA/MWNTs on filter paper were investigated with SEM. Figure 3a shows the porous network structure of carboxylated MWNTs. The carboxylated MWNTs alone were arranged as bundles due to the poor dispersion. The introduction of PDDA greatly resolved this aggregation problem, as confirmed by the well distribution of MWNTs on the paper substrates (Figure 3b).

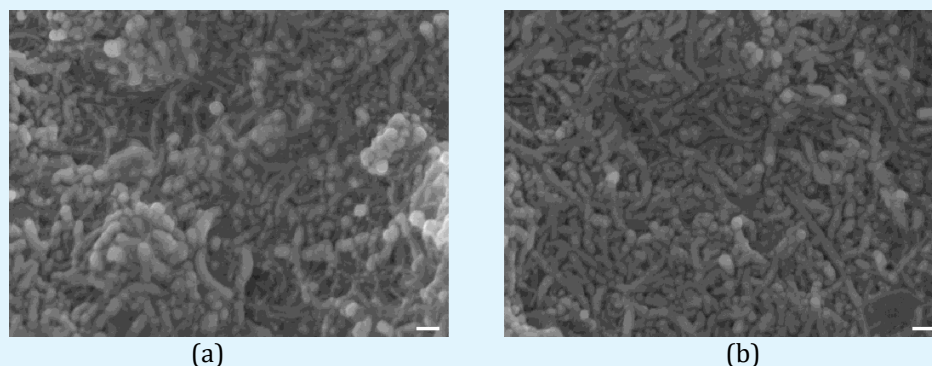


**Figure 3** SEM images of (a) carboxylated MWNTs, (b) PDDA/MWNTs electrode on paper. The Scale bar shows 100 nm.



### Electrochemical Behavior

Cyclic voltammetry (CV) is a commonly used technique for comparing and studying the behavior of the electrodes [25]. The electrochemical behavior of the PDDA/MWNTs were investigated using 5 mM  $[Fe(CN)_6]^{3-/4-}$  as the redox marker and compared with carboxylated MWNT electrode. As reflected by CV curves that both of MWNTs and PDDA/MWNTs paper electrodes exhibit a pair of quasi-reversible Faradic currents associated with the well-defined redox waves of the  $[Fe(CN)_6]^{3-/4-}$  couple, however, the Faradic current of PDDA/MWNTs are much larger than those of carboxylated MWNT paper electrode (Figure 4a), indicating that PDDA/MWNTs paper electrode substantially increases the electrochemical sensitivity of the system. Furthermore, the peak potential difference ( $\Delta E_p$ ) of the PDDA/MWNTs paper electrode ( $\Delta E_p = 0.38$ ; red line) decreases compared to the MWNTs ( $\Delta E_p = 0.42$ ; blue line), verifying that the polyelectrolyte functionalized MWNTs paper electrode accelerates electron transfer at the electrode. Upon functionalization

of the MWNTs with PDDA, both the onset potential and the oxidation peak potential of  $[Fe(CN)_6]^{3-/4-}$  shifted positively to around -0.18 V and 0.10 V, respectively, with the oxidation peak current of the  $[Fe(CN)_6]^{3-/4-}$  redox processes is ~1.2 times higher than observed at MWNTs paper electrode. This increased peak current at PDDA/MWNTs electrode is due to the preferential attraction of anionic probes by net positive charges created on carbon atoms in the nanotube carbon plane via intermolecular charge transfer with PDDA [21].

Figure 4b displays the voltammograms of PDDA/MWNTs paper electrode recorded at different scan rates. The anodic peak current,  $I_{pa}$  vs. square root of the scan rate,  $\nu$  (from 20 mV s<sup>-1</sup> to 150 mV s<sup>-1</sup>) plot (Figure 4b, inset) was highly linear ( $R^2 = 0.99$ );  $I_{pa} = -1.249 + 5.788\nu^{1/2}$ . The result verifies that the electrochemical kinetics is a diffusion-controlled oxidation process of redox probes.

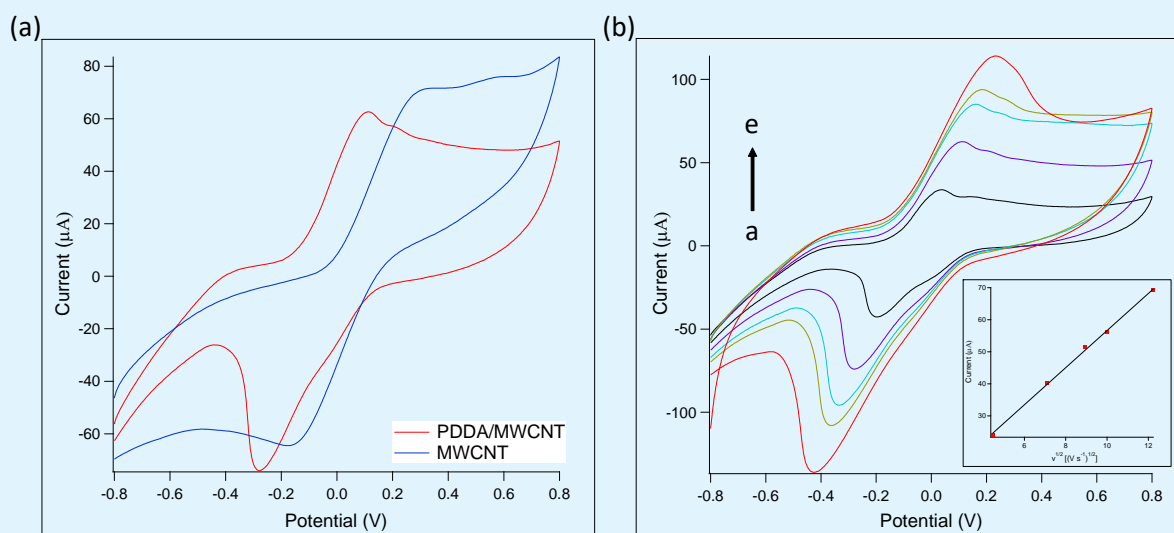


**Figure 4 (a):** Cyclic voltammograms of MWNTs and PDDA/MWNTs paper electrodes in 0.1 M PBS containing 5 mM  $[Fe(CN)_6]^{3-/4-}$ . Scan rate: 50 mV s<sup>-1</sup>; **(b)** Cyclic voltammograms of PDDA/MWNTs electrode at different scan rates: 20 mV s<sup>-1</sup>, 50 mV s<sup>-1</sup>, 80 mV s<sup>-1</sup>, 100 mV s<sup>-1</sup> and 150 mV s<sup>-1</sup>. Inset shows the dependence of anodic peak current of redox probes on scan rate.

### Electrochemical behavior of PDDA/MWNTs for DA in the presence of AA

Differential pulse voltammetry was employed to determine dopamine due to its higher current sensitivity and better resolution than cyclic voltammetry. Figure 5a

shows the DPVs recorded at PDDA/MWNTs electrode in 0.1 M phosphate buffer solution (black line) containing 1 mM AA (blue line) or 20 µM DA (black line). The oxidation potential of DA and AA were 0.12 V and -0.068 V, respectively. No oxidation peak was observed in blank

PBS solution. This suggests that PDDA/MWNTs electrode is useful to detect DA and AA. Furthermore, the two peaks separate well from each other making it possible to study the DA process and AA process independently. Knowing the electrochemical performance of PDDA/MWNT towards electrochemical discrimination of DA and AA, the influence of AA on the determination of DA was examined using DPVs. Figure 5b shows the DPV curves recorded in 0.1 M PBS containing 20  $\mu\text{M}$  DA and AA with various concentrations (0-500  $\mu\text{M}$ ). It was observed that the response of DA is much stronger than of AA. For example, the DA signal ( $\sim 1.2 \mu\text{A}$  for 20  $\mu\text{M}$ ) is over 6 times stronger than for AA ( $\sim 0.21 \mu\text{A}$ ), even though the AA concentration is up to 300  $\mu\text{M}$ , which could depress the interference from AA oxidation in determination of DA.

Furthermore, the peak potential separation ( $\Delta E_p$ ) between AA and DA was around 220 mV, suggesting the selective detection of PDDA/MWNTs towards DA. It was observed that the presence of AA increased the sensitivity of dopamine determination. This characteristic was also shown at a gold electrode modified with polypyrrole-mesoporous silica molecular sieves (polypyrrole-MCM-48) film [26]. The reason is that ascorbic acid is capable to reduce dopaquinone to dopamine, thus amplifying the oxidation current of dopamine at the surface electrode. The current response of AA exhibited a linear increase with AA concentration characterized by  $I_{pa} (\mu\text{A}) = -0.013 + 0.0008 C_{AA} (\mu\text{M})$  with a correlation of coefficient of 0.999 (Figure 5c).

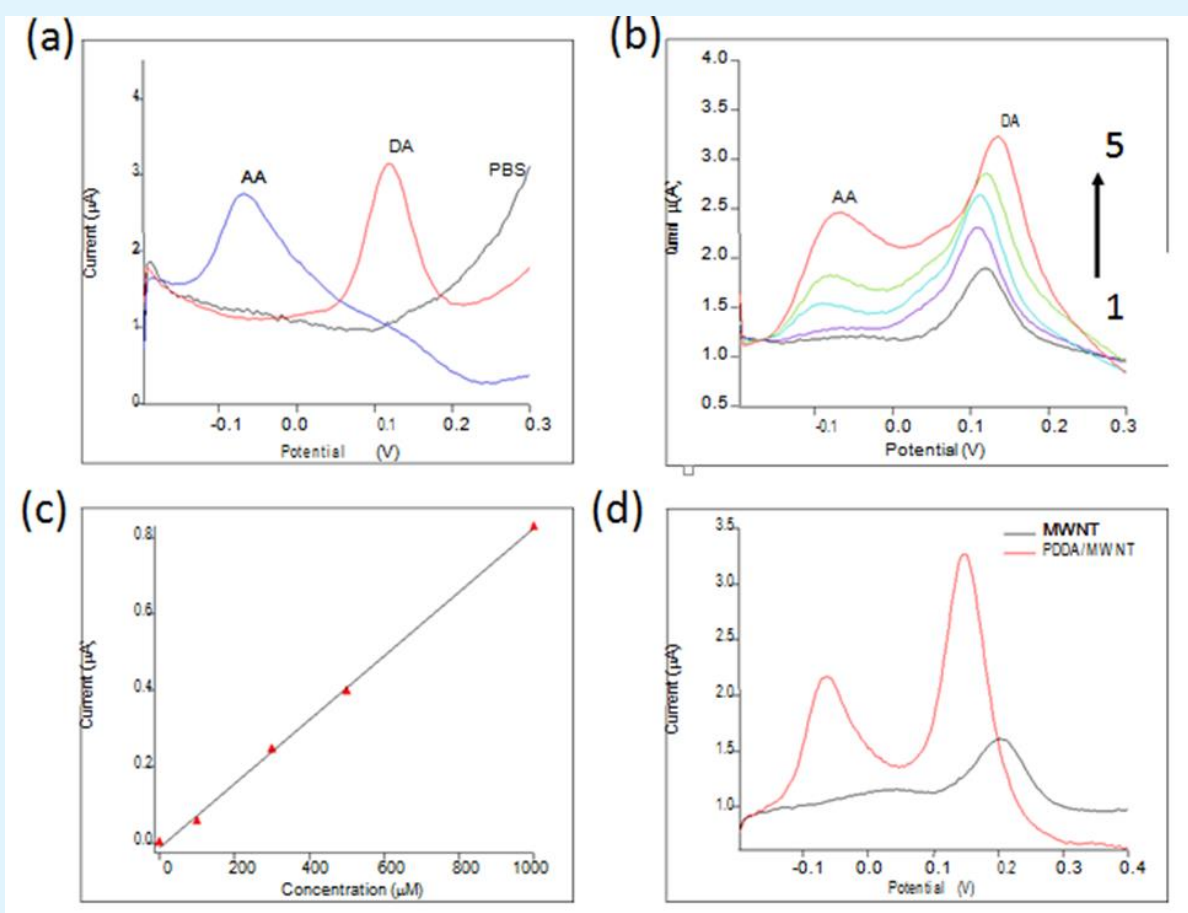


**Figure 5:** (a) DPVs recorded at PDDA/MWNTs paper electrode in 0.1 M PBS (black line) containing 1 mM AA (blue line), or 100  $\mu\text{M}$  DA (red line); (b) DPVs in 0.1 M PBS containing 20  $\mu\text{M}$  DA, and AA with concentrations: (1) 0 mM, (2) 0.1 mM, (3) 0.3 mM, (4) 0.5 mM, and (5) 1 mM; (c) A calibration plot of peak current vs AA concentration at PDDA/MWNTs electrode; (d) DPV of mixture solution containing 50  $\mu\text{M}$  DA and 1 mM AA in 0.1 M PBS at MWNTs (black line) and PDDA/MWNTs electrode (red line).

The electrochemical reactions of DA and AA at carboxylated MWNTs were also investigated and compared to PDDA/MWNTs in Figure 5d. The oxidation currents of AA and DA were 0.06  $\mu\text{A}$  and 0.5  $\mu\text{A}$  at 0.012 and 0.204 V for 1 mM AA and 100  $\mu\text{A}$  DA, respectively. The DA response at PDDA/MWNTs shows stronger signal (4.27  $\mu\text{A}$ ) and the oxidation peak potential is negatively shifted to 0.156 V compared to that for carboxylated MWNTs electrode. The increase in the oxidation peak currents and the lowering of oxidation peak potentials are clear evidence of the catalytic effect of PDDA/MWNTs towards DA and AA oxidation. The results agree with previous studies showing that increased electrochemical activity can be achieved at PDDA-graphene-multiwalled carbon nanotube glassy carbon electrode [27] and a nonaligned and vertically aligned CNTs with PDDA[28]. The MWNTs functionalized with PDDA also gives higher current response to negatively charges AA molecules, obtaining as high as 14.5 folds of that at the carboxylated MWNTs. The high sensitivity may be due to the combination of several positive attributes of PDDA/MWNTs [21]. PDDA absorbed onto MWNTs afforded the cationic nanotubes, hence negatively charged AA molecules are electrostatically attracted to the surface of PDDA/MWNT electrode. The PDDA/MWCNT provides a large specific surface area that improves both the ionic and electronic transport.

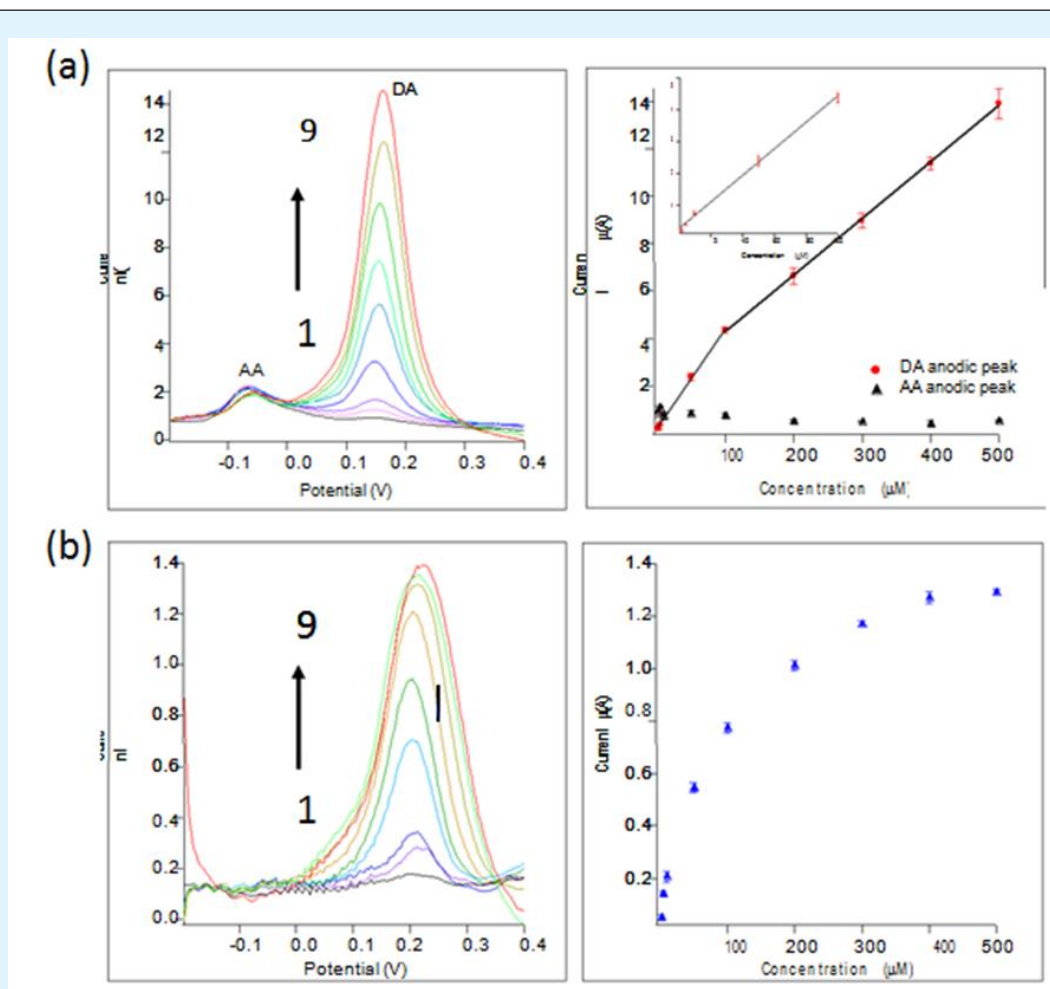
### Determination of DA at PDDA/MWNT by differential pulse voltammetry

Figure 6a shows the DPVs recorded for a mixture containing DA (2 – 500  $\mu\text{M}$ ) and AA (1 mM) in 0.1 M PBS solution at PDDA/MWNTs. Two separated peaks were observed and the calibration graphs were obtained. The oxidation peak currents of DA showed linear increases with lower region of DA concentration ranging from 2 to

100  $\mu\text{M}$  (Inset of figure 6a, right panel). The linear regression equation was  $I_{pa}(\mu\text{A}) = 0.207 + 0.042 C_{DA}(\mu\text{M})$ ,  $R^2 = 0.9985$ . The limit of detection (LOD) was calculated from the following relationship [29]:  $\text{LOD} = 3\sigma/s$ , where  $\sigma$  is the standard deviation of the peak current of the blank signal and  $s$  is the slope of the calibration plot. The detection limit for DA was estimated to be 0.8  $\mu\text{M}$ . Importantly, the oxidation currents of AA did not change with increase in DA concentration, indicating that PDDA/MWNT electrochemically detect DA in the presence of excess concentration of AA (1 mM). For the comparison, when using carboxylated MWNTs electrode under identical testing condition (Figure 6b), it is noted that the oxidation peak currents of DA is significantly lower than that of PDDA/MWNTs electrode. Furthermore, the oxidation peak currents of DA at oxidized MWNTs electrode shows a wider peak due to the overlapping of redox signal arising from the mixture of DA and AA. In addition, the oxidation peak current is saturated at 300  $\mu\text{M}$ . Such behaviors are attributed to fouling of oxidized MWNTs electrode [7]. Electrode fouling involves the passivation of an electrode surface by oxidized products of DA and AA. This passivation forms an increasing impermeable layer on the electrode, inhibiting the direct contact of DA with the electrode surface for electron transfer. By functionalized MWNTs with PDDA, electrode fouling is prevented. This effect is best displayed by the increased peak current for higher regions of DA concentration ranging from 100  $\mu\text{M}$  to 500  $\mu\text{M}$  (Figure 6a, right panel). The linear regression line is  $I_{pa}(\mu\text{A}) = 1.899 + 0.024 C_{DA}(\mu\text{M})$ ,  $R^2 = 0.9998$ . The existence of linear regression line for the two concentration regions (2-100  $\mu\text{M}$ , 100-500  $\mu\text{M}$ ) suggesting mechanism change of DA transport towards the PDDA/MWNTs electrode surface, from adsorptive to diffusional mode [10].

Electrode	Linear range	Detection	References
Cobalt salophen-modified carbon-paste electrode	1 $\mu\text{M}$ – 100 $\mu\text{M}$	0.5	(32)
PDDA/MWNT <sub>5</sub> /GC	2 $\mu\text{M}$ – 32 $\mu\text{M}$	-	(21)
O <sub>2</sub> plasma treated carbon nanotube nanoweb	1 $\mu\text{M}$ – 20 $\mu\text{M}$	-	(9)
carbon nanotube paste electrode of 2,2'-[1,2-ethanediylbis(nitriloethylidene)]-bis-hydroquinone	0.1 $\mu\text{M}$ – 900 $\mu\text{M}$	0.087	(33)
PPyox/graphene/GCE	0.5 $\mu\text{M}$ – 10 $\mu\text{M}$	0.1	(31)
CTAB functionalized graphene oxide (GO)/MWCNT/GCE	5 $\mu\text{M}$ – 500 $\mu\text{M}$	1.5	(34)
Au-CoP-Tyr	2 $\mu\text{M}$ – 60 $\mu\text{M}$	0.43	(30)
PDDA/MWCNT	2 $\mu\text{M}$ – 500 $\mu\text{M}$	0.8	This work
Cobalt salophen-modified carbon-paste electrode	1 $\mu\text{M}$ – 100 $\mu\text{M}$	0.5	(32)

**Table 1:** Comparison of linear range and detection limit of PDDA/MWNTs with other electrodes for DA.



**Figure 6:** Differential pulse voltammetry recorded at (a) PDDA/MWNTs and (b) carboxylated MWNT electrodes in 0.1 M phosphate buffer solution containing 1 mM AA and DA with various concentration: 2  $\mu\text{M}$ , 5  $\mu\text{M}$ , 10  $\mu\text{M}$ , 50  $\mu\text{M}$ , 100  $\mu\text{M}$ , 200  $\mu\text{M}$ , 300  $\mu\text{M}$ , 400  $\mu\text{M}$  and 500  $\mu\text{M}$ . The oxidation peak currents for AA is observed at PDDA/MWNTs but not at carboxylated MWNTs. The inset in figure shows a linear relationship for DA concentration from 2  $\mu\text{M}$  to 100  $\mu\text{M}$ . The oxidation peak currents for DA at carboxylated MWNTs is saturated at 300  $\mu\text{M}$ . Error bars indicates standard deviations for 5 independent experiments at each concentration.

The analytical performance of this PDDA/MWNTs paper electrode was compared with literature for measurement of DA (table 1). Compared with previous reports, the LOD obtained in this work is relatively low with a comparable linear range. Although Tyr-based sensor cross-linked on cobalt (II)-porphyrin (CoP) film [30] and overoxidized polypyrrole/graphene modified electrode [31-34] provided lower LODs, these systems are more complicated and expensive due to the requirement of enzyme and the large sample volume. The comparisons suggest that our paper electrode which can be fabricated

at lower cost could be a novel promising tool for DA detection.

## Conclusion

In summary, we demonstrated a simple fabrication method for making an array of PDDA/MWNTs electrode on a filter paper by lamination and drop-casting. The surface on paper can be made hydrophobic by fabric crayons drawn on paper. The PDDA/MWNTs electrodes show an excellent selectivity and sensitivity in detecting



DA in the presence of AA. In addition, all assays were performed with 10  $\mu$ l small sample volume without the use of pumps or external apparatus. By using DPV method, the limit of detection for DA is 0.8  $\mu$ M in the solution with excess AA mixture, which is comparable with results found in the literature for conducting polymer modified electrodes. Furthermore, there is a separation of  $\sim$ 220 mV between AA-DA peaks in the DPV plot, which was significant to clearly discriminate between the two substances. These results suggest the potential applicability of paper-based electrode for DA determination in real clinical practice.

### Author Contributions

“conceptualization, Tze-Sian Pui.; methodology, Yuan-Li Hoe and Than Aung; software, Tze-Sian Pui and Yuan-Li Hoe; validation, Tze-Sian Pui; resources, Tze-Sian Pui; data curation, Yuan-Li Hoe; writing—original draft preparation, Tze-Sian Pui; writing—review and editing, Yuan-Li Hoe, Song Wei Loo, Than Aung; supervision, Tze-Sian Pui; project administration, Song Wei Loo; funding acquisition, Tze-Sian Pui”

### Funding

This research was funded by Singapore Ministry of Education Academic Research Fund Tier 1 –(MOE-2018-T1-001-004)

### Acknowledgments

We thank the following people who kindly provided technical advice and other vital forms of support: Dr. Chen Peng (Instrumentation) and Chen Jie (SEM imaging).

**Conflicts of Interest:** “The authors declare no conflict of interest.”

### References

- Phillips PE, Stuber GD, Heien ML, Wightman RM, Carelli RM (2003) Subsecond dopamine release promotes cocaine seeking. *Nature* 422(6932): 614-618.
- Wilson GS, Johnson MA (2008) In-Vivo Electrochemistry: What Can We Learn about Living Systems? *Chem Rev* 108(7): 2462-2481.
- De Witte P (1996) The role of neurotransmitters in alcohol dependence: animal research. *Alcohol Alcohol Suppl* 31(1): 13-6
- García-Tornadú I, Ornstein AM, Chamson-Reig A, Wheeler MB, Hill DJ, et al. (2010) Disruption of the dopamine d2 receptor impairs insulin secretion and causes glucose intolerance. *Endocrinology*, 151(4): 1441-1450.
- Conway JF, Wikoff WR, Cheng N, Duda RL, Hendrix RW, et al. (2001) Virus Maturation Involving Large Subunit Rotations and Local Refolding. *Science* 292(5517): 744-748.
- Naranjo CA, Tremblay LK, Busto UE (2001) The role of the brain reward system in depression. *Prog Neuropsychopharmacol Biol Psychiatry* 25(4): 781-823.
- Alwarappan s, Liu G, Li CZ (2010) Simultaneous detection of dopamine, ascorbic acid, and uric acid at electrochemically pretreated carbon nanotube biosensors. *Nanomedicine* 6(1): 52-57.
- Khudaish EA, Al Farsi AA (2010) Electrochemical oxidation of dopamine and ascorbic acid at a palladium electrode modified with in situ fabricated iodine-adlayer in alkaline solution. *Talanta* 80(5): 1919-1925.
- Zhao J, Zhang W, Sherrell P, Razal JM, Huang XF, et al. (2012) *ACS Appl Mater Interfaces* 4: 44.
- Quan do P, Tuyen do P, Lam TD, Tram PT, Binh NH, et al. (2011) Electrochemically selective determination of dopamine in the presence of ascorbic and uric acids on the surface of the modified Nafion/single wall carbon nanotube/poly(3-methylthiophene) glassy carbon electrodes. *Colloids Surf B Biointerfaces* 88(2): 764-770.
- Roy PR, Okajima T, Ohsaka T (2003) Simultaneous electroanalysis of dopamine and ascorbic acid using poly (N,N-dimethylaniline)-modified electrodes. *Bioelectrochemistry* 59(1-2): 11-9.
- Raj CR, Ohsaka T (2001) Electroanalytical applications of cationic self-assembled monolayers: square-wave voltammetric determination of dopamine and ascorbate. *Bioelectrochemistry* 53(2):183-191.
- Wei D, Kvarnström C, Lindfors T, Ivaska A (2007) Electrochemical functionalization of single walled

- carbon nanotubes with polyaniline in ionic liquids. *Electrochemistry Communications* 9(2): 206-210.
14. Cao XH, Zhang LX, Cai WP, Li YQ (2010) *Electrochemistry Communications* 12: 540.
  15. Babaei A, Babazadeh M (2011) Multi-walled carbon nanotubes/chitosanpolymer composite modified glassy carbon electrode for sensitive simultaneous determination of levodopa and morphine. *Analytical Methods* 3: 2400-2405.
  16. Pui TS, Sudibya HG, Luan X, Zhang Q, Ye F, et al. (2010) Non-invasive detection of cellular bioelectricity based on carbon nanotube devices for high-throughput drug screening. *Advanced Materials* 22: 3199-3203.
  17. He W, Sun Y, Xi J, M Abdurhman AA, Ren J, et al. (2016) *Analytica Chimica Acta* 903: 61.
  18. Viry L, Derré A, Poulin P, Kuhn A (2010) *Physical Chemistry Chemical Physics* 12(34): 9959-9970.
  19. Komathi S, Gopalan AI, Lee KP (2009) Nanomolar detection of dopamine at multi-walled carbon nanotube grafted silica network/gold nanoparticle functionalised nanocomposite electrodes. *Analyst* 135(2): 397-404.
  20. Tashkhourian J, Nezhad MRH, Khodavesi J, Javadi S (2009) Silver nanoparticles modified carbon nanotube paste electrode for simultaneous determination of dopamine and ascorbic acid. *Journal of Electroanalytical Chemistry* 633(1): 85-91.
  21. Zhang M, Gong K, Zhang H, Mao L (2005) Layer-by-layer assembled carbon nanotubes for selective determination of dopamine in the presence of ascorbic acid. *Biosens Bioelectron* 20(7): 1270-1276.
  22. Manbohi A, Ahmadi SH (2019) Sensitive and selective detection of dopamine using electrochemical microfluidic paper-based analytical nanosensor. *Sensing and Bio-Sensing Research* 23: 100270.
  23. Punjiya M, Mostafalu P, Sonkusale S (2014) *IEEE Biomedical Circuits and Systems Conference (BioCAS) Proceedings*, pp: 324.
  24. López-Marzo AM, Merkoçi A (2016) Paper-based sensors and assays: a success of the engineering design and the convergence of knowledge areas. *Lab on a Chip* 16(17): 3150-3176.
  25. Xiao Y, Guo C, Li CM, Li Y, Zhang J, et al. (2007) Highly sensitive and selective method to detect dopamine in the presence of ascorbic acid by a new polymeric composite film. *Anal Biochem* 371(2): 229-237.
  26. Zablocka I, Wysocka-Zolopa M, Winkler K (2018) Electrochemical Detection of Dopamine at a Gold Electrode Modified with a Polypyrrole-Mesoporous Silica Molecular Sieves (MCM-48) Film. *Int J Mol Sci* 20(1): 111.
  27. He S, Yu Y, Chen Z, Shi Q, Zhang L (2015) *Analytical Letters* 48: 248.
  28. Wang S, Yu D, Dai L, Chang DW, Baek JB (2011) Polyelectrolyte-functionalized graphene as metal-free electrocatalysts for oxygen reduction. *ACS Nano* 5(8): 6202-6209.
  29. Hegde RN, Kumara Swamy BE, Shetti NP, Nandibewoor ST (2009) *Journal of Electroanalytical Chemistry* 635: 51.
  30. Florescu M, David M (2017) Tyrosinase-Based Biosensors for Selective Dopamine Detection. *Sensors (Basel)* 17(6): 1314.
  31. Liu Q, Zhu X, Huo Z, He X, Liang Y, et al. (2012) Electrochemical detection of dopamine in the presence of ascorbic acid using PVP/graphene modified electrodes. *Talanta* 97: 557-562.
  32. Amini MK, Khorasani JH, Khaloo SS, Tangestaninejad S (2003) Cobalt(II) salophen-modified carbon-paste electrode for potentiometric and voltammetric determination of cysteine. *Anal Biochem* 320(1): 32-38.
  33. Beitollahi H, Ardakani MM, Ganjipour B, Naeimi H (2008) Novel 2,2'-bis-hydroquinone double-wall carbon nanotube paste electrode for simultaneous determination of epinephrine, uric acid and folic acid. *Biosens Bioelectron* 24(3): 362-368.
  34. Yang YJ, Li W (2014) CTAB functionalized graphene oxide/multiwalled carbon nanotube composite modified electrode for the simultaneous determination of ascorbic acid, dopamine, uric acid and nitrite. *Biosens Bioelectron* 56: 300-306.

